Article title

Arabidopsis PFA-DSP-type phosphohydrolases target specific inositol pyrophosphate messengers

Philipp Gaugler[1§], Robin Schneider[1§], Guizhen Liu[2], Danye Qiu[2], Jonathan Weber[1], Jochen Schmid[3&], Nikolaus Jork[2,4], Markus Häner[2], Kevin Ritter[2], Nicolás Fernández-Rebollo[3], Ricardo F.H. Giehl[5], Minh Nguyen Trung[6], Ranjana Yadav[7], Dorothea Fiedler[6], Verena Gaugler[1], Henning J. Jessen[2], Gabriel Schaaf[1]*, Debabrata Laha[7]*

[1]Department of Plant Nutrition, Institute of Crop Science and Resource Conservation, Rheinische Friedrich-Wilhelms-Universität Bonn, 53115 Bonn, Germany

[2]Department of Chemistry and Pharmacy and CIBSS-Centre for Integrative Biological Signalling Studies, Albert-Ludwigs University Freiburg, 79104 Freiburg, Germany

[3]Center for Plant Molecular Biology, Department of Plant Physiology, Eberhard Karls University Tübingen, 72076 Tübingen, Germany

[4]Spemann Graduate School of Biology and Medicine (SGBM), University of Freiburg, 79104 Freiburg, Germany

[5]Department of Physiology & Cell Biology, Leibniz-Institute of Plant Genetics and Crop Plant Research, 06466 Gatersleben, Germany

[6]Leibniz-Forschungsinstitut für Molekulare Pharmakologie, 13125 Berlin, Germany; Department of Chemistry, Humboldt Universität zu Berlin, 12489 Berlin, Germany.

[7]Department of Biochemistry, Indian Institute of Science (IISc), Bengaluru-560012, India

[§]P.G. and R.S. contributed equally to this manuscript

*E-mail: gabriel.schaaf@uni-bonn.de, dlaha@iisc.ac.in

ORCID IDs: P.G.: 0000-0002-9187-404X, R.S. 0000-0002-9657-4548, G.L. 0000-0003-1748-6687, DQ: 0000-0003-2197-3218, J.S.: 0000-0001-7527-7088, N.J.: 0000-0002-3717-443X, M.H.: 0000-0003-3313-4868, K.R.: 0000-0001-7900-1855, N.F.R.: 0000-0003-3556-8766, R.F.H.G: 0000-0003-1006-3163, M.N.T.: 0000-0003-3100-9609, R.Y.: 0000-0003-4956-5638, D.F.: 0000-0002-0798-946X, V.G.: 0000-0002-3249-2922, H.J.J: 0000-0002-1025-9484, GS: 0000-0001-9022-4515, D.L.: 0000-0002-7823-5489

Short title

A. thaliana inositol pyrophosphate phosphohydrolases

ABSTRACT

Inositol pyrophosphates are signaling molecules containing at least one phosphoanhydride bond that regulate a wide range of cellular processes in eukaryotes. With a cyclic array of phosphate esters and diphosphate groups around *myo*-inositol, these molecular messengers possess the highest charge density found in nature. Recent work deciphering inositol pyrophosphate biosynthesis in *Arabidopsis* revealed important functions of these messengers in nutrient sensing, hormone signaling and plant immunity. However, despite the rapid hydrolysis of these molecules in plant extracts, very little is known about the molecular identity of the phosphohydrolases that convert these messengers back to their inositol polyphosphate precursors. Here, we investigate whether *Arabidopsis* Plant and Fungi Atypical Dual Specificity Phosphatases (PFA-DSP1-5) catalyze inositol pyrophosphate phosphohydrolase activity. We find that recombinant proteins of all five *Arabidopsis* PFA-DSP homologs display phosphohydrolase activity with a high specificity for the 5-β-phosphate of inositol pyrophosphates. We further show that heterologous expression of *Arabidopsis* PFA-DSP1-5 rescues wortmannin-sensitivity and deranged inositol pyrophosphate homeostasis caused by the deficiency of the PFA-DSP-type inositol pyrophosphate phosphohydrolase Siw14 in yeast. Heterologous expression in *Nicotiana benthamiana* leaves provided evidence that *Arabidopsis* PFA-DSP1 also displays 5-β-phosphate specific inositol pyrophosphate phosphohydrolase activity *in planta*. Our findings lay the biochemical basis and provide the genetic tools to uncover the roles of inositol pyrophosphates in plant physiology and plant development.

INTRODUCTION

Inositol pyrophosphates (PP-InsPs), such as $InsP_7$ and $InsP_8$, are molecules derived from *myo*-inositol (Ins) esterified with unique patterns of monophosphates (P) and diphosphates (PP), and have been described as versatile messengers in yeast, amoeba, and animal cells [1-4]. With recent discoveries that PP-InsPs regulate nutrient sensing and immunity in plants, these molecules are a novel focus of research in plant physiology [5-13]. The synthesis of PP-InsPs is partially conserved in eukaryotes, with some important distinctions in plants. In baker's yeast and mammals, 5-$InsP_7$ is synthesized by Kcs1/IP6K-type proteins whereas Vip1/PPIP5K-type

kinases phosphorylate the C1 position of both $InsP_6$ (also termed phytic acid) and $5\text{-}InsP_7$, generating $1\text{-}InsP_7$ and $1,5\text{-}InsP_8$, respectively [14-17]. In plants, detection, quantification and characterization of PP-InsPs have been challenging due to the low abundance of these molecules and their susceptibility to hydrolytic activities during extraction [18, 19]. Employing [³H] *myo*-inositol labelling and subsequent analysis of plant extracts by strong-anion exchange high performance liquid chromatography (SAX-HPLC) allowed the detection of PP-InsPs in different plant species [5, 20-22]. The recent development of capillary electrophoresis (CE) electrospray ionization mass spectrometry (ESI-MS), has enabled the detection and quantification of many InsP and PP-InsP isomers in various cell extracts including all $InsP_7$ isomers, except enantiomers (labeled e.g. as 1/3 or 4/6 $InsP_7$) [23]. Similar to yeast and mammals, the *Arabidopsis* PPIP5K isoforms, VIH1 and VIH2 catalyse the synthesis of $InsP_8$ [5, 10] and are likely involved in the synthesis of $1/3\text{-}InsP_7$ [11]. However, Kcs1/IP6K-type proteins are absent in land plants. The question of how plants synthesize $5\text{-}InsP_7$ has been partially solved by work on *Arabidopsis* inositol (1,3,4) triphosphate 5/6 kinases ITPK1 and ITPK2. Notably, ITPK1 and ITPK2 were reported to catalyse the synthesis of $5\text{-}InsP_7$ from $InsP_6$ *in vitro* [24-26] and consequently *itpk1* mutant plants display reduced $5\text{-}InsP_7$ levels [11, 13].

In *Arabidopsis*, disturbances in the synthesis of $InsP_7$ and/or $InsP_8$ result in defective signaling of the plant hormones jasmonate [5, 6] and auxin [13], as well as defects in salicylic acid-dependent plant immunity [12] and impaired phosphate (P_i) homeostasis [9-11, 27]. In the case of auxin and jasmonate perception, $5\text{-}InsP_7$ and $InsP_8$, respectively, are proposed to function as co-ligands of the respective receptor complexes [5, 6, 13]. The role of PP-InsPs in P_i signaling are related to their ability to bind to SPX proteins, which act as receptors for these messenger molecules [7, 9, 10, 28-30]. $InsP_8$ has been found as the preferred ligand for stand-alone SPX proteins *in vivo* [9, 10, 28]. $InsP_8$-bound SPX receptors inactivate the MYB-type transcription factors PHR1 and PHL1, which control the expression of a majority of P_i starvation-induced (PSI) genes to regulate various metabolic and developmental adaptations induced by P_i deficiency [28, 31-33]. The tissue levels of various PP-InsPs, including $5\text{-}InsP_7$ and $InsP_8$, respond sensitively to the plant's P_i status [9, 11], suggesting that their synthesis and degradation are tightly regulated. While the steps involved in the synthesis of PP-InsPs in plants are now better understood, still little is known about how these molecules are degraded.

Vip1/PPIP5Ks are bifunctional enzymes that harbour an N-terminal ATP-grasp kinase domain and a C-terminal phosphatase domain conserved in yeast, animals and plants [5, 10, 15, 17, 34]. *In vitro*, the phosphatase domain of *Arabidopsis* PPIP5K VIH2 hydrolyses PP-InsPs to $InsP_6$ [10], similar to the respective C-terminal domains of fission yeast and mammalian PPIP5Ks [35, 36]. Although *Arabidopsis* ITPK1 harbors no phosphatase domain, under conditions of low adenylate charge it can shift its activity *in vitro* from kinase to ADP phosphotransferase activity using $5\text{-}InsP_7$ but no other $InsP_7$ isomer [11, 26]. Apart from relying on the reversible activities of ITPK1 and Vip1/PPIP5Ks, the degradation of PP-InsPs may also be controlled by specialized phosphohydrolases.

In mammalian cells, diphosphoinositol polyphosphate phosphohydrolases (DIPPs), members of the nudix hydrolase family, have been shown to catalyse hydrolysis of the diphosphate groups of $InsP_7$ and $InsP_8$ at the C1 and C5 position [4, 37, 38]. The baker's yeast genome encodes a single homologue of mammalian DIPP1, named diadenosine and diphosphoinositol polyphosphate phosphohydrolase (DDP1), which hydrolyses various substrates including diadenosine polyphosphates, $5\text{-}InsP_7$ and $InsP_8$, but has a preference for inorganic polyphosphates (poly-P) and for the β-phosphate of $1\text{-}InsP_7$ [39-41]. In addition, baker's yeast has an unrelated PP-InsP phosphohydrolase, Siw14 (also named Oca3) with a high specificity for the β-phosphate at position C5 of $5\text{-}InsP_7$ [42, 43]. This enzyme is a member of the Plant and Fungi Atypical Dual Specificity Phosphatases (PFA-DSPs) that belong to a large family of protein tyrosine phosphatases (PTPs) [43-45].

Blast search analyses revealed that the *Arabidopsis thaliana* genome encodes five PFA-DSPs, with AtPFA-DSP1 sharing 61% identity and 76% similarity with yeast Siw14 [44, 45]. X-ray crystallography revealed that the protein adopts an α/β fold typical for cysteine phosphatases, with the predicted catalytic cysteine (Cys150) residing at the bottom of a positively-charged pocket [44, 46]. Of a number of putative phosphatase substrates tested, recombinant AtPFA-DSP1 displayed the highest activity against inorganic polyphosphate, as well as against deoxyribo- and ribonucleoside triphosphates, and less activity against phosphotyrosine-containing peptides and phosphoinositides [46]. Here, we investigated whether *Arabidopsis* PFA-DSPs might function as PP-InsP phosphohydrolases.

Results and Discussion

Arabidopsis PFA-DSP proteins display *in vitro* PP-InsP phosphohydrolase activity with high specificity for 5-InsP$_7$

To explore a potential role of *Arabidopsis* PFA-DSP proteins in PP-InsP hydrolysis, we firstly generated translational fusions of PFA-DSPs with an N-terminal hexahistidine tag followed by a maltose binding protein (MBP) and expressed recombinant proteins in bacteria. Corresponding His-MBP-Siw14 and free His-MBP constructs were generated as controls. All constructs allowed the purification of soluble recombinant proteins (Figure S1). We then tested potential PP-InsP phosphohydrolase activities of PFA-DSP1 with 1-InsP$_7$ or 5-InsP$_7$ in the presence of various divalent cations. Notably, PFA-DSP1 failed to catalyze the hydrolysis of 1-InsP$_7$ or 5-InsP$_7$ in the presence of Mn^{2+}, Ca^{2+} or Zn^{2+}. However, in the presence of the cytoplasmic prevalent cation Mg^{2+}, PFA-DSP1 displayed a robust hydrolytic activity against 5-InsP$_7$, likely resulting in the generation of InsP$_6$, as deduced from the mobility of the reaction product separated by polyacrylamide gel electrophoresis (PAGE) and visualized by toluidine blue staining (Figure 1A). CE-ESI-MS analysis of the reaction product spiked with a [^{13}C$_6$] InsP$_6$ standard confirmed that the resulting product indeed had the migration behavior and the mass of phytic acid (Figure 1B). In contrast, 1-InsP$_7$ was largely resistant to PFA-DSP1 also in the presence of Mg^{2+} (Figure 1A). In the absence of divalent cations (i.e. in buffer not supplemented with divalent cations but instead supplemented with EDTA, a condition unlikely to represent any cellular condition) both InsP$_7$ isomers were hydrolyzed to InsP$_6$, as deduced from the mobility of the reaction product by PAGE (Figure 1A).

We then tested the hydrolytic activities of the *Arabidopsis* PFA-DSP homologs with all six 'simple', synthetic InsP$_7$ isomers and with the two enantiomeric InsP$_8$ isomers 1,5-InsP$_8$ and 3,5-InsP$_8$ in the presence of Mg^{2+}. Of note, *myo*-inositol is a meso compound with a mirror plane dissecting the C2 and C5 position. Derivatives differentially (pyro)phosphorylated at the C1 and C3 position, as well as at the C4 and C6 position are enantiomeric forms that can only be distinguished in the presence of appropriate chiral selectors [47, 48]. Yeast Siw14 and all *Arabidopsis* PFA-DSPs with the exception of PFA-DSP5, displayed robust activity with a high specificity towards 5-InsP$_7$ (Figure 1C), confirming earlier reports that 5-InsP$_7$ is a preferred substrate for yeast Siw14 as compared to 1-InsP$_7$ [42, 43]. PFA-DSP1-4 and Siw14 also displayed

partial hydrolytic activities against the enantiomers 4-InsP$_7$ and 6-InsP$_7$, as well as very weak hydrolytic activities against enantiomeric 1-InsP$_7$ and 3-InsP$_7$ (Figure 1C). The latter activities were more pronounced in PFA-DSP1 and PFA-DSP3 as compared to Siw14 and PFA-DSP2. As for 5-InsP$_7$, the reaction products with the other InsP$_7$ isomers had the mass and the migration behavior of the InsP$_6$ isomer phytic acid, as deduced from CE-ESI-MS analyses (Figures 1D and S2).
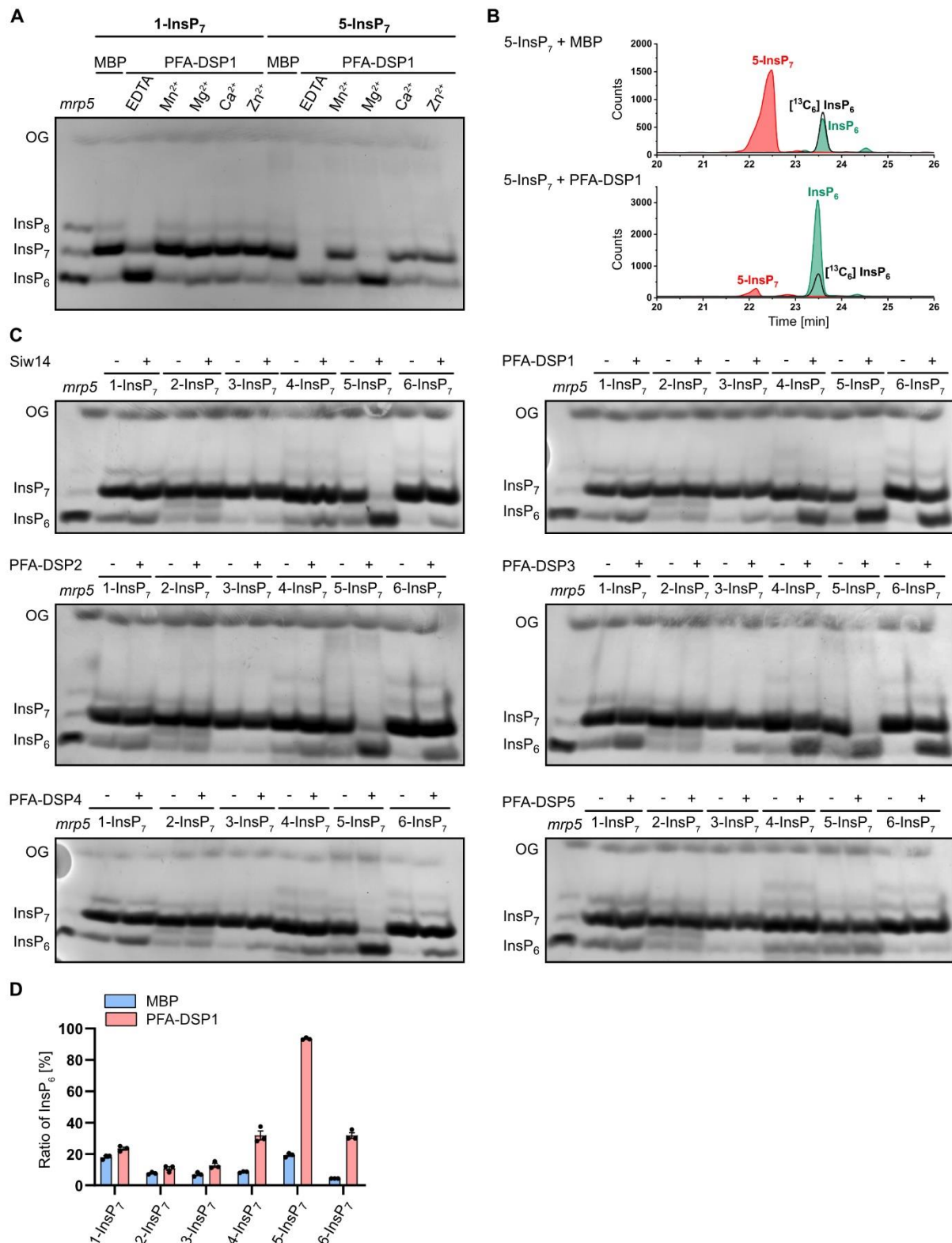
Figure 1: *In vitro*, *Arabidopsis* PFA-DSPs display Mg^{2+}-dependent PP-InsP phosphohydrolase activity with high specificity for 5-InsP$_7$. Recombinant His-MBP-DSPs and His-MBP-Siw14 were incubated with 0.33 mM InsP$_7$ for 1 h at 22°C. His-MBP served as a negative control. (A) 0.4 μM His-MBP-DSP1 was incubated with 1-InsP$_7$ or 5-InsP$_7$ and either 1 mM EDTA, MnCl$_2$, MgCl$_2$, CaCl$_2$ or ZnCl$_2$ as indicated. The reaction products were then separated by 33 % PAGE and visualized by toluidine blue. (B-D) The InsP$_7$ phosphohydrolase activity of approximately 0.4 μM His-MBP-DSPs and His-MBP-Siw14 was analyzed

in presence of 1 mM $MgCl_2$. The reaction products were then (B, D) spiked with isotopic standards mixture ($[^{13}C_6]$1,5-$InsP_8$, $[^{13}C_6]$5-$InsP_7$, $[^{13}C_6]$1-$InsP_7$, $[^{13}C_6]$ $InsP_6$, $[^{13}C_6]$2-OH $InsP_5$) and subjected to CE-ESI-MS analyses or (C) separated by 33 % PAGE and visualized by toluidine blue/DAPI staining. (D) Data represent means ± SEM (n = 3). Representative extracted-ion electropherograms are shown in Figure S2.

Notably, PFA-DSP5 only showed very weak activities at the 0.4 µM concentration tested in our assay. However, when the reaction time was extended from 1 h to 2 h and the enzyme concentration was increased to 2 µM, PFA-DSP5 displayed robust activity with a substrate specificity similar to PFA-DSP1-4 and yeast Siw14, with a high selectivity for 5-$InsP_7$ and only weak hydrolytic activities against 4-$InsP_7$ and 6-$InsP_7$ (Figure 2A). Notably, the meso $InsP_7$ isomer 2-$InsP_7$ was completely resistant to Siw14 or any of the *Arabidopsis* PFA-DSP proteins under the assay conditions. This was also the case in the absence of divalent cations (i.e. in buffer not supplemented with divalent cations but instead supplemented with EDTA), where Siw14 and *Arabidopsis* PFA-DSP1-4 failed to hydrolyze 2-$InsP_7$ to a significant extent while all other $InsP_7$ isomers were at least partially converted to an InsP isomer with the mobility of phytic acid (Figures S3 and S4). Even after a 24 h-long incubation with *Arabidopsis* PFA-DSP1, 2-$InsP_7$ remained largely resistant to hydrolysis. In contrast, all other PP-$InsP_7$ isomers were hydrolyzed to $InsP_6$ under these conditions, as revealed by PAGE and CE-ESI-MS analyses (Figures 2B,C and S5). Corresponding control reactions that were supplemented with 5-$InsP_7$ after 23 h validated the activity of *Arabidopsis* PFA-DSP1 after such long incubation times (Figures 2C and S6). These spiking experiments also rules out the possibility that 2-$InsP_7$ contained a contaminant that inhibits PFA-DSP-dependent hydrolysis, as 5-$InsP_7$ was still efficiently hydrolyzed in the presence of 2-$InsP_7$.
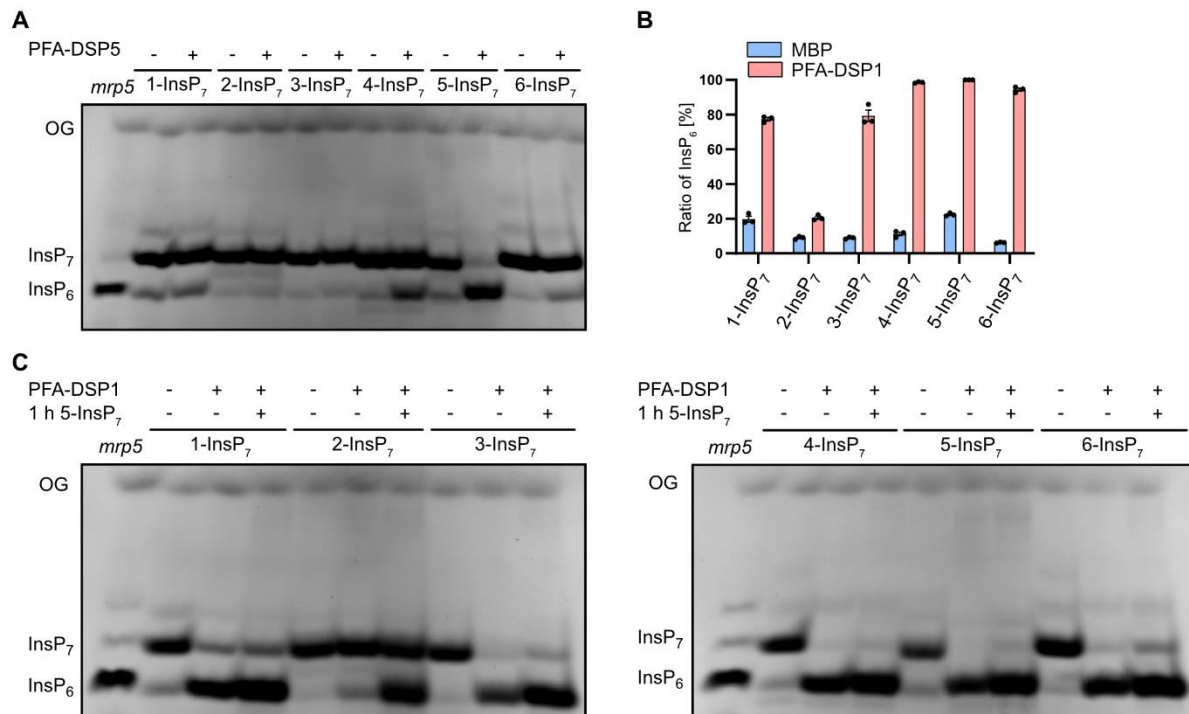
Figure 2: Under prolonged incubation times and/or at increased protein concentrations, selected *Arabidopsis* **PFA-DSPs hydrolyze various InsP₇ isomers** *in vitro*, **except for 2-InsP₇.** Recombinant His-MBP-DSPs or His-MBP-Siw14 were incubated with 1 mM $MgCl_2$ at 22°C. His-MBP served as a negative control. (A) 2 µM recombinant His-MBP-DSP5 was incubated with 0.33 mM $InsP_7$ isomers for 2 h and the reaction product was separated by 33 % PAGE and visualized with toluidine blue. (B, C) 0.4 µM PFA-DSP1 was incubated with 0.33 mM $InsP_7$ for 24 h. To ensure that PFA-DSP1 is active during the whole incubation time, after 23 h, 0.33 mM 5-$InsP_7$ was added to a replicate and incubated for another 1 h. (B) An aliquot of the reaction product was spiked with an isotopic standards mixture ($[^{13}C_6]$1,5-$InsP_8$, $[^{13}C_6]$5-$InsP_7$, $[^{13}C_6]$1-$InsP_7$, $[^{13}C_6]$ $InsP_6$, $[^{13}C_6]$2-OH $InsP_5$) and subjected to CE-ESI-MS analyses. Data represent means ± SEM (n = 3). (C) Another reaction was separated by 33 % PAGE and visualized with toluidine blue. Representative extracted-ion electropherograms are shown in Figure S5.

Finally, we tested whether the enantiomeric $InsP_8$ isomers 1,5-$InsP_8$ and 3,5-$InsP_8$ serve as substrates for PFA-DSPs. As reported earlier for Siw14 [43], PFA-DSP1-4 hydrolyzed 1,5-$InsP_8$ to an $InsP_7$ isomer based on the mobility of the reaction product in PAGE analyses (Figure 3A). Also the enantiomeric 3,5-$InsP_8$ was efficiently hydrolyzed by Siw14 and PFA-DSP1-4 (Figure 3A) and CE-ESI-MS analysis of the reaction products showed the migration behavior and the mass of 1/3-$InsP_7$ (Figures 3B,C and S7).

Altogether, these findings reveal that *Arabidopsis* PFA-DSP proteins, as well as Siw14 have a high specificity for the 5-β-phosphate of 5-$InsP_7$, 1,5-$InsP_8$ and 3,5-$InsP_8$, and a weak activity

against the β-phosphates of 4-InsP$_7$ and 6-InsP$_7$, respectively. In contrast, InsP$_6$ and 2-InsP$_7$ are resistant to PFA-DSP-catalyzed hydrolysis.
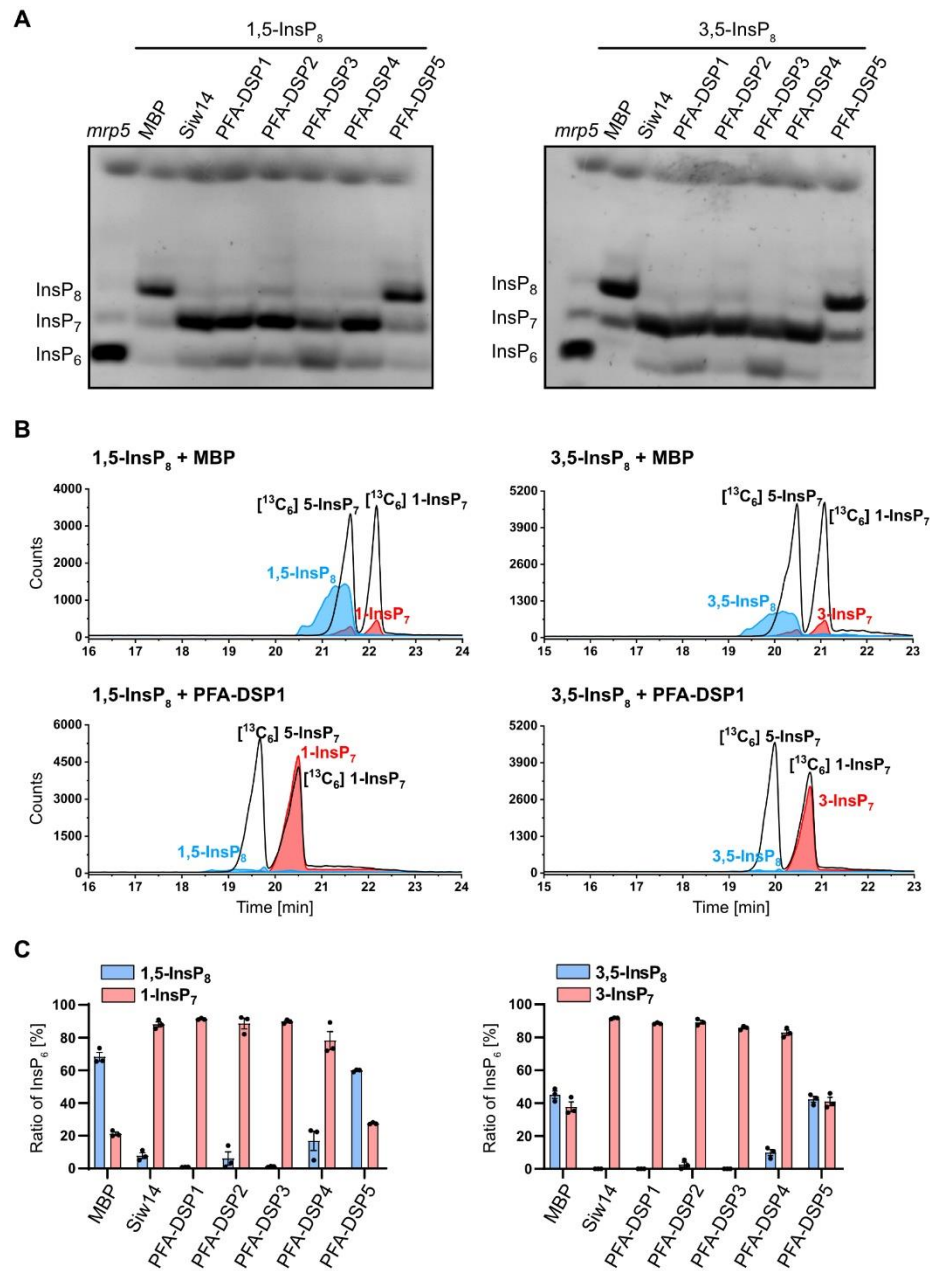
Figure 3: *In vitro*, *Arabidopsis* **PFA-DSPs display robust 1/3,5-InsP$_8$ phosphohydrolase activity.** (A) Approximately 0.4 µM His-MBP-DSPs and His-MBP-Siw14 were incubated with 0.33 mM 1,5-InsP$_8$ or 3,5-InsP$_8$ for 1 h, in presence of 1 mM MgCl$_2$, and analyzed by PAGE and subsequent toluidine blue staining. (B, C) A second and third reaction were spiked with isotopic standards mixture ([^{13}C$_6$]1,5-InsP$_8$, [^{13}C$_6$]5-InsP$_7$, [^{13}C$_6$]1-InsP$_7$, [^{13}C$_6$] InsP$_6$, [^{13}C$_6$]2-OH InsP$_5$) and subjected to CE-ESI-MS analyses. (C) Data represent means ± SEM (n = 3). Representative extracted-ion electropherograms are shown in Figure S7.

Heterologous expression of *Arabidopsis PFA-DSP* homologs complement yeast *siw14Δ* defects

To investigate the physiological consequences of *Arabidopsis* PFA-DSP activities *in vivo*, we carried out heterologous expression experiments in baker's yeast. To this end, we first screened the *siw14Δ* yeast strain for phenotypes and identified a not yet described severe growth defect on media containing the fungal toxin wortmannin [49]. Previous observations that *kcs1Δ* yeast cells are resistant to wortmannin [50] suggest that wortmannin sensitivity of *siw14Δ* yeast might be related to Kcs1-dependent PP-InsPs. The *siw14Δ* -associated growth defect was fully complemented by heterologous expression of either of the five *Arabidopsis PFA-DSP* homologs or of yeast *SIW14* from episomal plasmids under control of a *PMA1* promotor fragment (Figure 4A). To investigate the contribution of PFA-DSPs in InsP metabolism, we monitored InsP profiles using SAX-HPLC analyses of various $[^3H]$-*myo*-inositol labelled yeast transformants. Of note, conventional SAX-HPLC analyses as employed here do not allow the discrimination of different $InsP_7$ or $InsP_8$ isomers [11, 48]. Heterologous expression of PFA-DSPs in *siw14Δ* restored $InsP_7/InsP_6$ ratios to wild-type levels, indicating that *Arabidopsis* PFA-DSP proteins are functionally similar to Siw14 (Figure 4B).
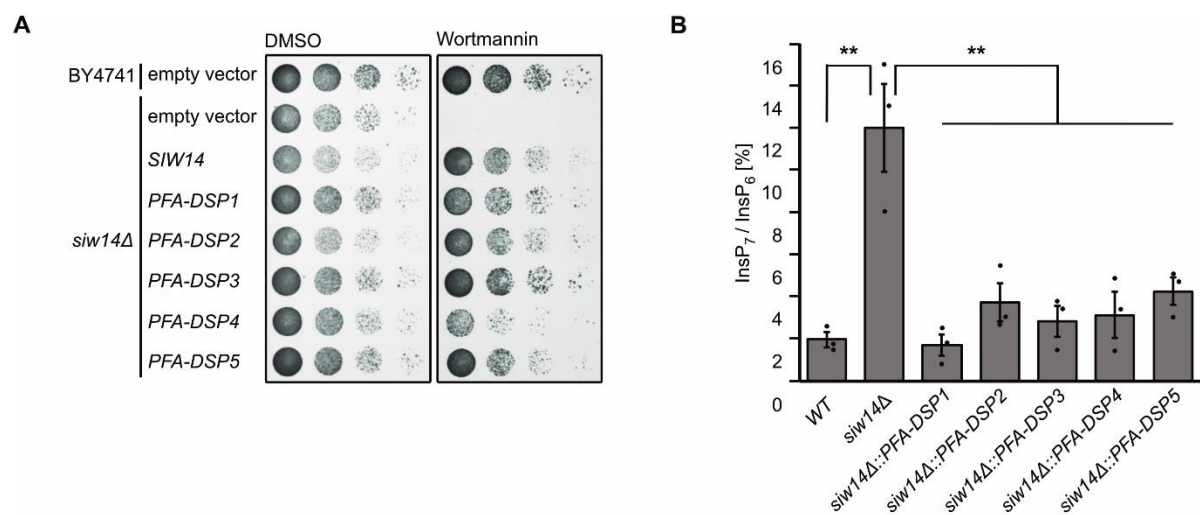
Figure 4: Heterologous expression of *Arabidopsis* PFA-DSPs complements *siw14Δ*-associated wortmannin sensitivity in yeast. (A) Growth complementation assays of an *siw14Δ* yeast strain. Wild-type yeast (BY4741) and an isogenic *siw14Δ* yeast mutant were transformed with either the empty episomal pDRf1-GW plasmid or with different pDRf1-GW plasmids carrying the respective *PFA-DSP* gene or *SIW14*. Yeast transformants were then spotted in 8-fold serial dilutions (starting from OD$_{600}$ 1.0) onto selective media supplemented with either wortmannin or DMSO as control. Plates were incubated at 26 °C for 2 days before photographing. The yeast growth assay was repeated twice (n =

3) with similar results. (B) The relative amounts of InsP$_7$ of wild-type yeast, *siw14Δ* and *siw14Δ* transformed with pDRf1-GW carrying the *DSP* genes are shown as InsP$_7$/InsP$_6$ ratios. InsP$_6$ and InsP$_7$ levels were determined by analysis of SAX-HPLC profiles using OriginPro 8. Data represent means ± SEM (n = 3). Asterisks indicate values that are significantly different from *siw14Δ* (according to Student's *t* test, P<0.05 (*); P<0.01 (**); P<0.001 (***)).

Notably, the InsP$_7$ signal was the only one consistently affected by the loss of *SIW14* and heterologous expression of any *PFA-DSP* gene (Figure S8). We generated variants of Siw14 or PFA-DSP1, in which the catalytic cysteine was replaced by a serine resulting in a C214S and a C150S substitution in Siw14 and PFA-DSP1, respectively, and observed that complementation of *siw14Δ*-associated growth defects of respective transformants requires the catalytic activity of these proteins (Figures S9A,B). The inability of catalytic dead mutants to complement *siw14Δ* -associated growth defects was not caused by compromised expression or protein stability of these variants, as confirmed by immunoblot analyses (Figure S9C). In agreement with the growth complementation assays, the catalytically inactive versions of Siw14 and PFA-DSP1 also failed to restore wild-type InsP$_7$ levels in *siw14Δ* transformants (Figures S9D,E). These experiments suggest that *Arabidopsis* PFA-DSPs can substitute for endogenous Siw14 in yeast with respect to wortmannin tolerance and InsP$_7$ homeostasis and that complementation of the *siw14Δ*-associated defects depends on the catalytic activity of these proteins.

Growth defects of *siw14Δ* yeast on wortmannin require Kcs1-dependent 5-InsP$_7$ synthesis

For a deeper understanding of the wortmannin phenotype of *siw14Δ* yeast, we investigated genetic interactions between Siw14 and different InsP kinases. We generated different double mutants with defects in Siw14 and the PP-InsP synthases Kcs1 and Vip1, and tested their performance on wortmannin-containing media (Figure 5A). Again, *siw14Δ* cells did not survive on media supplemented with 3 μM wortmannin, a defect that was fully complemented by the expression of *SIW14* under control of the endogenous promoter from a *CEN*-based single copy plasmid (Figure 5A). Growth of *vip1Δ* cells was comparable to wild-type yeast. In contrast, the *vip1Δ siw14Δ* double mutant showed a severe growth defect on media supplemented with wortmannin similar to single *siw14Δ* cells (Figure 5A). Like the

vip1Δ yeast strain, a *kcs1Δ* strain did not show growth defects on media supplemented with wortmannin as compared to control media. In contrast, at increased concentrations we observed *kcs1Δ*-associated wortmannin resistance (Figure 5B), as reported earlier [50]. Importantly, deletion of *KCS1* in *siw14Δ* cells rescued *siw14Δ*-associated wortmannin sensitivity since the resulting *kcs1Δ siw14Δ* double mutant yeast strain, despite growing overall weaker than the *kcs1Δ* single mutant strain, showed no increased sensitivity to wortmannin (Figure 5A). These findings indicate that the presence of Kcs1 is critical for the growth defects displayed by *siw14Δ* single mutant cells on wortmannin. We then investigated whether the presence of Kcs1 itself or of Kcs1-dependent PP-InsPs such as 5-InsP$_7$ are relevant for *siw14Δ*-associated wortmannin sensitivity. To this end, we examined the phenotypes of *ipk2Δ* and of *ipk2Δ siw14Δ* yeast transformants. Both mutants lack IPK2, an inositol polyphosphate multikinase that sequentially phosphorylates Ins(1,4,5)P$_3$ to Ins(1,3,4,5,6)P$_5$ and is hence required for InsP$_6$ and subsequent Kcs1-dependent 5-InsP$_7$ or PP-InsP$_4$ synthesis [50, 51]. Neither of the strains showed growth defects on media supplemented with wortmannin as compared to the isogenic wild-type yeast strain, suggesting that also the loss of *IPK2* rescues *siw14Δ*-associated wortmannin sensitivity (Figure 5A). We further tested wortmannin sensitivity of *kcs1Δ* and *kcs1Δ siw14Δ* yeast transformants in a different genetic background and observed similar results (Figures 5B,C). Taken together, these results provide a causal link between Kcs1- (but not Vip1-) dependent PP-InsPs and *siw14Δ* -associated wortmannin sensitivity with Kcs1 and Siw14/PFA-DSPs playing antagonistic roles in regulating this sensitivity.
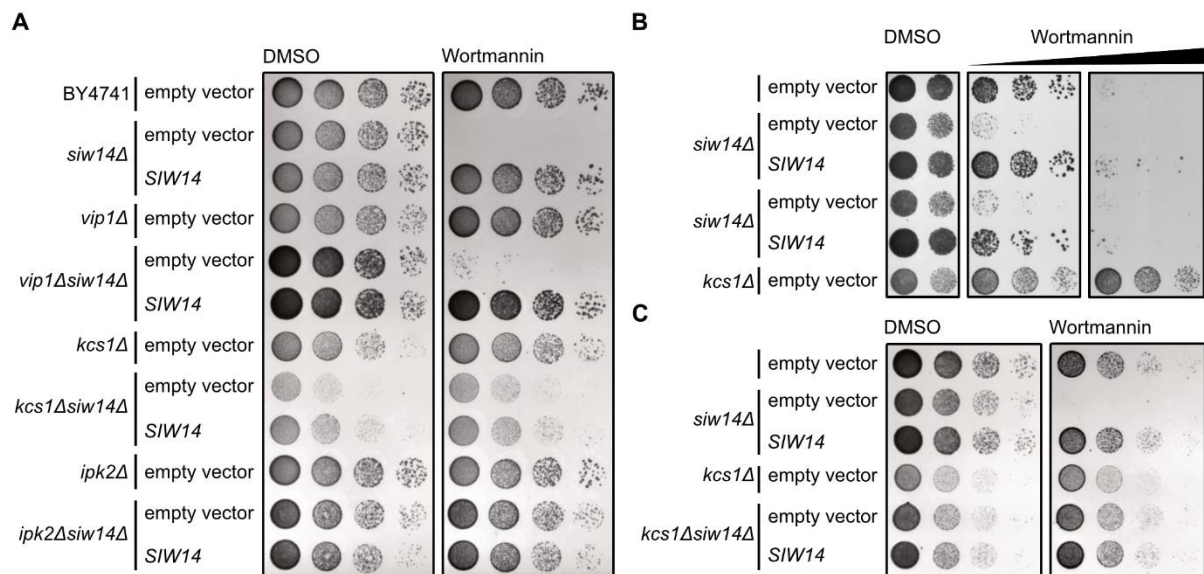
Figure 5: Yeast *siw14Δ*-associated wortmannin sensitivity requires Kcs1-dependent 5-InsP$_7$. (A) A Wild-type yeast (BY4741), *siw14Δ*, *vip1Δ*, *kcs1Δ*, *ipk2Δ*, *vip1Δ siw14Δ*, *kcs1Δ siw14Δ* and *ipk2Δ siw14Δ* double mutant yeast strains were transformed with either empty YCplac33 vector or with a YCplac33 vector carrying a genomic fragment of *SIW14* including a 653 bp promoter and 5'UTR and a 289 bp terminator region. Yeast transformants were then spotted in 8-fold serial dilutions (starting from OD$_{600}$ 1.0) onto selective media supplemented with either wortmannin or DMSO as control. Plates were incubated at 26 °C for 2 days before photographing. (B,C) Wild-type yeast (DDY1810), *siw14Δ*, *kcs1Δ* and (C) *kcs1Δ siw14Δ* double mutant yeast strains were transformed with either empty YCplac33 vector or with a YCplac33 vector carrying the genomic fragment of *SIW14*. The growth assay was performed as described for (A). All yeast growth assays (A - C) were repeated twice (n = 3) with similar results.

Increased *PFA-DSP1* expression coincides with decreases InsP$_7$ levels *in planta*

To gain insight into DSP functions *in planta*, we searched for *Arabidopsis* T-DNA insertion lines of *PFA-DSP1* and were able to identify three lines, *pfa-dsp1-3* and *pfa-dsp1*-6 in the Col-0 background and *pfa-dsp1-4* in the Ler-0 background, for which homozygous progeny could be obtained. None of these lines displayed an obvious growth phenotype under our standard growth conditions. SAX-HPLC profiles of extracts of 20-days old [^{3}H]-*myo*-inositol labeled *pfa-dsp1-3* and *pfa-dsp1-4* seedlings did not reveal a significant difference compared to the respective wild-types (Figures S10A,B). However, SAX-HPLC analyses of the *pfa-dsp1-6* line revealed a significant average reduction (around 36%) of the InsP$_7$/InsP$_6$ ratio compared to Col-0 (Figure 6B). The levels of other InsP species remained largely unaffected (Figure 6A). The available sequencing data for this line, as well as our analysis, indicated that the insertion of the T-DNA is 18 bp upstream of the start codon, suggesting that the full-length transcript

and DSP1 protein might be expressed in this line. We therefore conducted qPCR analyses of *pfa-dsp1-6* seedlings that were grown under identical conditions as the seedlings for SAX-HPLC analyses and detected an approximately 6-fold increased expression of *PFA-DSP1* in *pfa-dsp1-6* in comparison to Col-0 seedlings (Figure 6C).
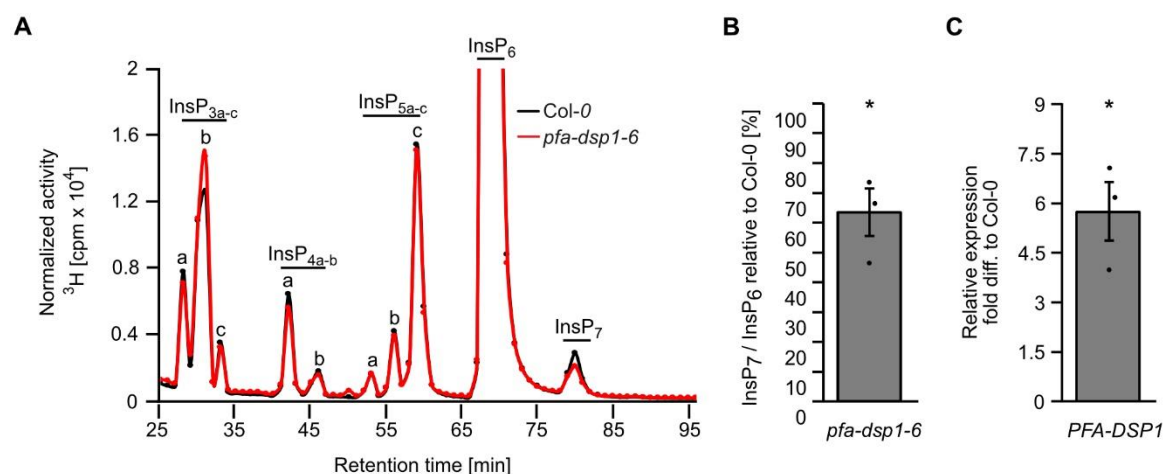
Figure 6: Increased expression of *PFA-DSP1* in *Arabidopsis* decreases InsP$_7$ levels. (A) A representative SAX-HPLC profile of 20-days-old wild-type (Col-0) and *pfa-dsp1-6 Arabidopsis* seedlings radiolabeled with [^{3}H]-*myo*-inositol. All visible peaks are highlighted and assigned to the corresponding InsP species. Based on published chromatographic mobilities [52, 53], InsP$_{4a}$ likely represents Ins(1,4,5,6)P$_4$ or Ins(3,4,5,6)P$_4$, InsP$_{5a}$ likely represents InsP$_5$ [2-OH], InsP$_{5b}$ likely represents InsP$_5$ [4-OH] or its enantiomeric form InsP$_5$ [6-OH], and InsP$_{5c}$ likely represents InsP$_5$ [1-OH] or its enantiomeric form InsP$_5$ [3-OH]. The isomeric natures of InsP$_{3a-c}$, InsP$_{4b}$, InsP$_7$, and InsP$_8$ are unknown. (B) InsP$_7$/InsP$_6$ ratio of *dsp1-6* relative to Col-0 determined by analysis of SAX-HPLC profiles using OriginPro 8. (C) Relative expression of *PFA-DSP1* in plants grown under identical conditions as for SAX-HPLC analyses, presented as fold difference compared to Col-0. (B, C) Data represent means ± SEM (n = 3). Asterisks indicate values that are significantly different from the control (according to Student's *t* test, P<0.05 (*); P<0.01 (**); P<0.001 (***)).

Since the analyses of the *pfa-dsp1-6* line indicated that the T-DNA insertion causes an overexpression of *PFA-DSP1*, resulting in decreased InsP$_7$ levels, we investigated whether PP-InsP phosphohydrolase activity is also observed in a heterologous plant expression system. To this end, we transiently expressed a translational fusion of PFA-DSP1 with a C-terminal EYFP under control of the strong viral CaMV *35S* promoter in *Nicotiana benthamiana* using agrobacterium-mediated transfection. The respective catalytically inactive PFA-DSP1^{C150S}-EYFP fusion protein was also expressed and InsPs were then extracted from *Nicotiana*

benthamiana leaves and purified by TiO$_2$ pulldown 5 days after infiltration. PAGE analyses showed that transient expression of DSP1 or expression of its catalytic inactive version did not alter InsP$_6$ levels (Figure 7A). In contrast, InsP$_7$ levels were reduced by the transient expression of PFA-DSP1 but not by expression of its catalytic inactive version (Figure 7A). These findings were strengthened by subsequent CE-ESI-MS analyses that revealed no changes in the ratios of 1/3-InsP$_7$/InsP$_6$ or 4/6-InsP$_7$/InsP$_6$ as compared to control leaves infiltrated with agrobacteria carrying the silencing inhibitor *P19* alone (Figure 7B). In contrast, the 5-InsP$_7$/InsP$_6$ ratio was significantly reduced in plants expressing *PFA-DSP1* compared to plants expressing the inactive version of *PFA-DSP1* or *P19* alone. The InsP$_8$/InsP$_6$ ratio, in turn, was strongly reduced by the expression of *PFA-DSP1* in agreement with a partial hydrolytic activity of DSP proteins against InsP$_8$ isomers (Figures 3 and S7) and in agreement with the finding that 5-InsP$_7$, a substrate hydrolyzed by PFA-DSP1, represents the major precursor for InsP$_8$ synthesis [11]. In summary, these results demonstrate that ectopic expression of *Arabidopsis PFA-DSP1* results in a specific decrease of 5-InsP$_7$ and InsP$_8$ *in planta*.
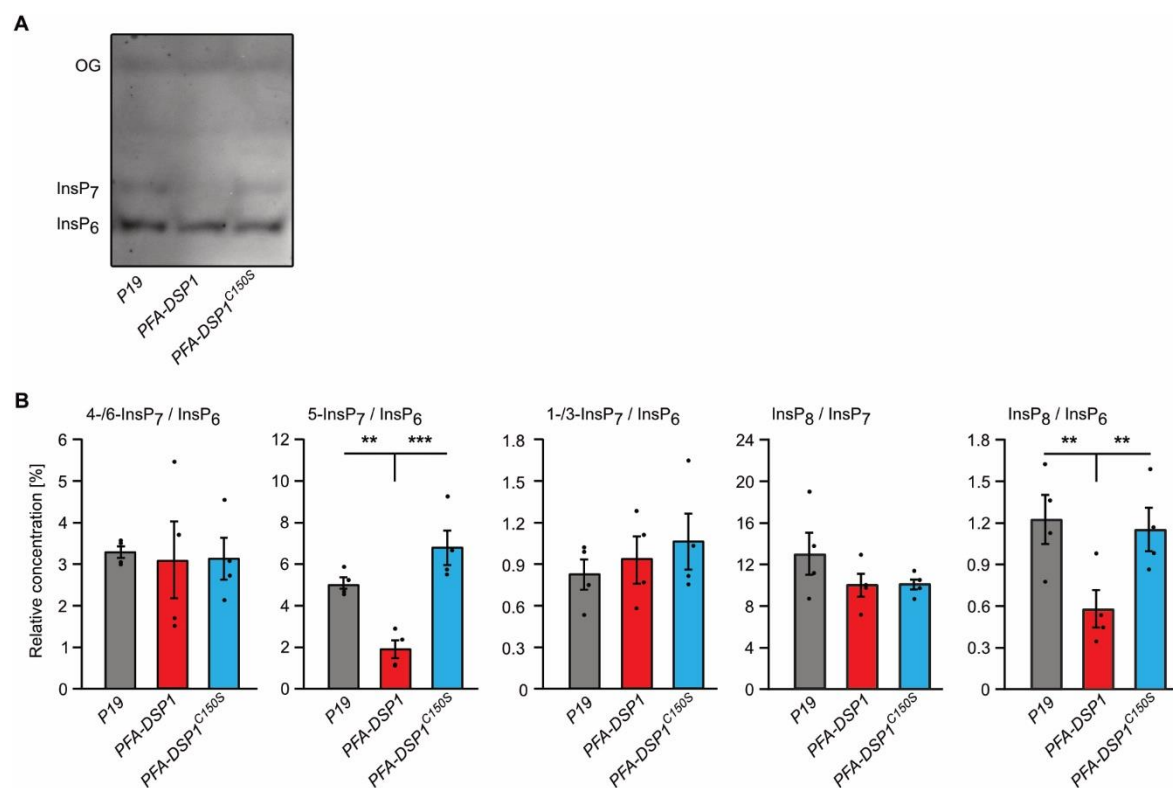
Figure 7: Transient expression of *PFA-DSP1* in *Nicotiana benthamiana* leaves specifically decreases 5-InsP$_7$ and InsP$_8$. InsPs from infiltrated *Nicotiana benthamiana* leaves, transiently expressing the

silencing inhibitor *P19* alone or together with *DSP1-EYFP* or *DSP1[C150S]-EFYP*, were purified with TiO_2 pulldown and analyzed using CE-ESI-MS. Detected peaks were assigned to specific InsP isomers and quantified by comparing them with ^{13}C InsP standards that were spiked into the purified samples. (A) A representative PAGE gel of a sample set used for CE-ESI-MS analysis. (B) Relative amounts of PP-InsPs compared to $InsP_6$ or of $InsP_8$ compared to all $InsP_7$ isomers as indicated. Data represent means ± SEM (n = 4). Asterisks indicate values that are significantly different from wild-type (according to Student's *t* test, P<0.05 (*); P<0.01 (**); P<0.001 (***)). Note that 4- or 6-$InsP_7$, as well as 1- or 3-$InsP_7$ represent enantiomeric forms that cannot be distinguished by CE-ESI-MS analyses.

Conclusions

Recent studies elucidating the identity and substrate specificity of $InsP_6$/PP-InsP kinases have allowed to establish important functions of PP-InsPs in nutrient sensing, hormone signaling and plant immunity [5-13, 20, 28]. In contrast, information on enzymatic activities removing PP-InsPs to switch off their signaling functions in plants is sparse. Intriguingly, the first robust detection of PP-InsP messengers in mammalian cells was made possible by blocking mammalian PP-InsP phosphohydrolases with fluoride [1]. While substantial progress in elucidating the role of various PP-InsP phosphohydrolases in regulating these messengers in yeast and mammalian cells has been made [37, 41, 42, 54], we are unaware of any study about PP-InsP degrading enzymes in plants on the onset of this study. Here, we provide evidence that the *Arabidopsis* PFA-DSP proteins are functional homologs of yeast Siw14 with high phosphohydrolase specificity for the 5-β-phosphate of various PP-InsPs.

The striking biochemical similarities between *Arabidopsis PFA-DSPs* as deduced from *in vitro* assays and heterologous expressions analyses in yeast might well explain redundancies of these enzymes and consequently a lack of obvious phenotypes in single *pfa-dsp* loss-of-function lines in *Arabidopsis*. A search in transcriptome studies revealed that *PFA-DSP1*, *2* and *4* are strongly induced by P_i deficiency (Figure S11). Such P_i-dependent regulation is in line with the disappearance of PP-InsPs in tissues of P_i-starved plants (Dong et al., 2019; Riemer et al., 2021), but future studies are required to establish the involvement on PFA-DSPs in the removal of messengers controlling P_i signaling. The high specificity of PFA-DSPs observed in this study establishes these enzymes as ideal tools to investigate the physiological roles of 5-β-phosphate containing PP-InsPs in plant development, plant immunity, nutrient perception and abiotic stress tolerance. This is particularly important because of potentially confounding effects caused by the recently discovered plant 4/6-$InsP_7$ [11], but also because higher order

mutants involved in the synthesis of 5-β-phosphate containing PP-InsPs such as *itpk1 itpk2* and *vih1 vih2* display severe developmental defects or die at young seedling stage [10, 11]. With the availability of a variety of promoters with tight spatial and temporal regulation, ectopic expression of *PFA-DSPs* in a tissue and developmentally controlled manner will provide helpful insights to unravel the roles of 5-InsP$_7$ and 1/3, 5-InsP$_8$ in plant development and plant physiology.

Methods

Plant materials and growth conditions

Seeds of *Arabidopsis thaliana* T-DNA insertion lines *pfa-dsp1-3* (WiscDsLox_473_B10, Col-0), *pfa-dsp1-4* (CSHL_GT1415, Ler-0) and *pfa-dsp1-6* (SAIL_116_C12, Col-0) were obtained from The European Arabidopsis Stock Centre (http://arabidopsis.info/). In order to identify homozygous lines, F2 and F3 plants were genotyped by PCR using the primers indicated in Table S1.

For sterile cultures, *Arabidopsis* seeds were surface sterilized in 1.2 % (v/v) NaHClO$_4$ and 0.05 % (v/v) Triton X-100 for 3 min, in 70 % (v/v) ethanol and 0.05 % (v/v) Triton X-100 for 3 min and in 100 % (v/v) ethanol before transferring onto sterile filter paper. Sterilized seeds were sown onto half-strength Murashige and Skoog (MS) medium [55] containing 1 % sucrose, pH 5.7 and solidified with 0.7 % (w/v) Phytagel (Sigma-Aldrich). After 2 days of stratification at 4°C, the plates were transferred to a growth incubator and the seedlings were grown under short-day conditions with the following regime: 8/16 h light/dark; light intensity 120 µmol m^{-2} s^{-1}; temperature 22 °C/20 °C.

Constructs

The following full-length ORFs were amplified by PCR from an *Arabidopsis* whole seedling cDNA preparation: *PFA-DSP1* (At1g05000), *PFA-DSP2* (At2g32960), *PFA-DSP3* (At3g02800) *PFA-DSP4* (At4g03960), and *PFA-DSP5* (At5g16480). Likewise, the *SIW14* ORF sequence was amplified from yeast genomic DNA. Primers used for amplification are listed in Table S1. The reverse primers contained a *V5* sequence (underlined) allowing a translational fusion of the resulting gene products with a C-terminal V5 epitope tag. Amplification products were cloned into pDONR221 (Invitrogen) via BP clonase II (Invitrogen) reaction following the manufacturer's instructions. The ORFs were then swapped into the episomal yeast expression

vector pDRf1-GW [56] by the LR clonase II (Invitrogen) reaction following the manufacturer's instructions. For expression of *SIW14* under control of the endogenous promoter from a *CEN*-based plasmid, the *SIW14* gDNA was amplified from purified yeast gDNA using primers listed in Table S1. The *SIW14* gDNA was inserted into YCplac33 (ATCC #87586) using the restriction enzymes *Pst*I and *Eco*RI.

For protein expression, *PFA-DSP1 – 5* were amplified as described before but with a reverse primer containing a stop codon. Amplified products were cloned into pDONR221 (Invitrogen), then swapped by LR clonase II (Invitrogen) into the bacterial expression vector pDEST566 (Addgene plasmid # 11517), which contains a sequence encoding an N-terminal His_6-maltose binding protein (MBP) epitope tag. Free His-tagged MBP protein was expressed from a modified pET28 vector carrying an N-terminal sequence encoding a His_8-maltose binding protein (MBP) epitope tag [5].

For transient expression in *Nicotiana benthamiana*, the ORF of *PFA-DSP1* (wild-type sequence and with a mutated sequence encoding the C150S substitution) was swapped by LR clonase II (Invitrogen) from pDONR221 into the plant expression vector pGWB641 [57], which harbors a viral CaMV *35S* promoter to allow gene expression and a sequence encoding a C-terminal EYFP tag. Site-directed mutagenesis was performed on the respective plasmids with primers listed in Table S1.

Nicotiana benthamiana infiltration

A single colony of transformed *Agrobacteria* was inoculated in 2 mL LB media containing the appropriate antibiotics and cultivated overnight at 26°C in a spinning wheel. On the next morning, 1 mL of overnight culture was added to 5 mL fresh LB with antibiotics and grown for another 4 h at 26°C. Afterwards, the cultures were harvested by centrifugation at 4°C with 3000 *g* for 20 min. The pellet was then resuspended in 3 mL infiltration solution containing 10 mM $MgCl_2$, 10 mM MES-KOH (pH 5.6) and 150 µM acetosyringone. OD_{600} was determined using a 1:10 dilution and adjusted to 0.8 in infiltration solution. Then the working solution was prepared by pooling equal amounts of cultures that were co-infiltrated (e.g. *P19* + *PFA-DSP1*). The abaxial surface of the leaf (lower side) was then infiltrated using a 1 mL syringe without a needle. Afterwards, the plants were placed in a dark incubator at 26°C for approx. 1 day before keeping them for another 4 days on the workbench. The leaves were then harvested and frozen in liquid nitrogen before continuing with the extraction of inositol phosphates.

Yeast Strains

Different strains of the budding yeast *Saccharomyces cerevisiae* were used. The BY4741 wild-type (MATa *his3Δ leu2Δ met15Δ ura3Δ*), *siw14Δ* (*YNL032w::kanMX4*), *vip1Δ* (*YLR410w::kanMX4*), *kcs1Δ* (*YDR017c::kanMX4*), and *ipk2Δ* (*YDR173c::kanMX4*) were obtained from Euroscarf. *vip1Δ siw14Δ, kcs1Δ siw14Δ, ipk2Δ siw14Δ* were generated by using *loxP*/Cre gene disruption and the *ble* resistance marker, which confers phleomycine/Zeocin (Invitrogen) resistance [58] using primers listed in Table S1. In addition, the following mutants in the DDY1810 background (MATa; *leu2Δ ura3-52 trp1Δ; prb1-1122 pep4-3 pre1-451*) [59] were used: *kcs1Δ* and *kcs1Δ ddp1Δ. kcs1Δ siw14Δ, kcs1Δ ddp1Δ siw14Δ* and *siw14Δ* were generated in this background as described before. For all assays, the yeast cells were transformed by the Li-acetate method [60] and cultured either in 2 x YPD + CSM medium or selective synthetic deficiency (SD) medium.

Yeast growth complementation assay

Yeast transformants were inoculated in selective synthetic deficiency (SD) medium and grown overnight at 28°C while shaking (200 rpm). Then the OD_{600} was measured, adjusted to 1.0 and an 8-fold dilution series was prepared in a 96-well plate. Subsequently, 10 µL of each dilution were spotted on selective solid media as described earlier [61] and incubated at 26°C for 2 - 4 days. To prepare selective solid media supplemented with wortmannin, autoclaved media was cooled down to 60°C, wortmannin was added from a 10 mM stock in DMSO (Sigma Aldrich) to a final concentration of 1 - 3 µM. Since the activity of wortmannin changed by age and by the number of freezing/thawing cycles, aliquots were kept at -20°C and were not thawed more than five times. In addition, several concentrations were employed for the spotting assays to be able to identify the activity at which growth differences between *siw14Δ, kcs1Δ* and their isogenic wildtype transformants became most obvious. Pictures were taken with a Bio-Rad ChemiDoc MP imager using white backlight.

Protein preparation

His$_6$-MBP-PFA-DSP protein fusions or free His$_8$-MBP were expressed in *Escherichia coli* BL21 CodonPlus (DE3)-RIL cells (Stratagene). Overnight bacterial cultures were inoculated 1:1000 into fresh 2YT medium (1.6 % tryptone, 1 % yeast extract, 0.5 % NaCl) with 100 mg/L ampicillin (pDEST566) or 50 mg/L kanamycin (pET28) and 25 mg/L chloramphenicol. Cells were grown at 37°C while shaking (200 rpm) for 4 h (approx. 0.6 OD_{600}), and protein expression was induced at 16°C overnight with 0.1 mM isopropyl-D-1-thiogalactopyranoside. Cells were lysed as described [62] using the following lysis buffer: 50 mM Tris-Cl, pH 7.5, 100 mM NaCl, 25 mM

imidazole, 10 % (v/v) glycerol, 0.1 % (v/v) Tween 20, 5 mM β-mercaptoethanol and the EDTA-free complete ULTRA protease inhibitor cocktail (Roche). Proteins were batch-purified using Ni-NTA agarose resin (Macherey-Nagel) and eluted using the abovementioned lysis buffer with increased imidazole concentration (250 mM). Three elutions were combined and dialyzed using Slide-A-Lyzer™ Dialysis Cassettes (Thermo Scientific) following the manufacturer's instructions and a buffer containing 50 mM Tris-Cl, pH 7.5 and 100 mM NaCl. The concentrated protein preparations were then stored at -20 °C. Purified proteins were analyzed using SDS-PAGE followed by Coomassie blue staining. Proteins were compared with PageRuler plus prestained protein ladder (Thermo Fisher) and with designated amounts of a BSA standard to estimate target protein concentrations.

In vitro PP-InsP phosphohydrolase assay

The phosphohydrolase assay was carried out in a 15 µl reaction mixture containing 0.35 µM – 2 µM recombinant PFA-DSP or Siw14 protein, 50 mM HEPES (pH 7.0), 10 mM NaCl, 5 % (v/v) glycerol, 0.1 % (v/v) β-mercaptoethanol and 0.33 mM of various $InsP_7$ and $InsP_8$ isomers as indicated, and was incubated for 1 h, 2 h or 24 h at 22°C. The PP-InsP isomers were synthesized as described previously [63, 64]. Reactions were separated by 33% PAGE and visualized by toluidine blue or DAPI staining.

Titanium dioxide bead extraction and PAGE/CE-ESI-MS

Purification of inositol polyphosphates using TiO_2 beads and analysis via PAGE was performed as described previously [11]. CE-ESI-MS analyses of *in vitro*, yeast and plant samples were performed as described previously [11, 23].

Inositol polyphosphate extraction from yeast cells and seedlings and HPLC analyses

For inositol polyphosphate analyses from yeast, transformants were inoculated into selective synthetic deficiency (SD) medium and grown overnight at 28 °C while shaking (200 rpm). They were then diluted 1:200 in 2 mL fresh medium supplemented with 6 µCi mL^{-1} [^{3}H]-*myo*-inositol (30–80 Ci mmol^{-1}; Biotrend; ART-0261-5) and grown overnight at 28°C in a spinning wheel. After harvest of the cell pellet, inositol polyphosphates were extracted and analysed as described before [5, 65, 66].

Extraction of [^{3}H]-*myo*-inositol polyphosphates from *Arabidopsis* seedlings and subsequent SAX-HPLC analyses were performed as described previously [66].

RNA isolation and quantitative real-time PCR

15-days old seedlings were transferred from solid half-strength MS plates to liquid half-strength MS media (supplemented with 1 % sucrose) for 5 days before harvest and immediately frozen in liquid N_2. Total RNA was extracted with NuceloSpin RNA Plant and Fungi kit (Macherey-Nagel). cDNA was synthesized using RevertAid RT reverse transcription kit (Thermo Fisher). Quantitative PCR reactions were conducted with the CFX384 real-time system (Bio-Rad) and the SsoAdvanced Universal SYBR Green Supermix (Bio-Rad) using the primers listed in Table S1. *TIP41like* and *PP2AA3* were used as reference genes to normalize relative expression levels of all tested genes. Relative expression was calculated using the CFX Maestro software (Bio-Rad).

Yeast protein extraction and immunodetection

Multiple transformants were inoculated into 4 mL of YPD (with 3 % glucose) or selective SD-media and grown for up to 24 h at 28°C. On the following day, the yeast was re-inoculated into 4 mL fresh media and grown for another day. Afterwards the cells were harvested and resuspended in 500 µL extraction buffer (300 mM sorbitol, 150 mM NaCl, 50 mM Na_2HPO_4, 1 mM EDTA, pH 7.5), supplemented with 100 mM β-mercaptoethanol and a 1:50 dilution of protease inhibitor cocktail for fungal extracts (Sigma-Aldrich). Cells were lysed with bead beating using 150 – 200 µL of glass beads (ø 0.5 mm). Lysate was spun down and the supernatant boiled for 10 min after addition of sample buffer. The protein extracts were then resolved by SDS-PAGE. Target proteins were detected by immunoblot. As primary antibody a mouse anti-V5 (Invitrogen, R960-25, 1:2000 dilution) antibody was used, followed by an Alexa fluor plus 800 goat anti-mouse antibody (Invitrogen, 1:20000 dilution). As loading control, Gal4 was detected using a rabbit polyclonal anti-Gal4 antibody (Santa Cruz, 1:1000 dilution), followed by a goat anti-rabbit StarBright Blue 700 antibody (Bio-Rad, 1:2500 dilution). The signal was detected using the multi-plex function of the ChemiDoc MP imager (Bio-Rad)

Accession numbers

DNA and Protein Sequences can be obtained from the Saccharomyces Genome database (https://www.yeastgenome.org/), TAIR (https://www.arabidopsis.org) and UniProt (https://www.uniprot.org/) under the following accession numbers: *SIW14* (YNL032W, NC_001146.8), *Arabidopsis PFA-DSP1* (At1g05000, NM_100379.3), *Arabidopsis PFA-DSP2* (At2g32960, NM_128856.5), *Arabidopsis PFA-DSP3* (At3g02800, NM_111148.3), *Arabidopsis PFA-DSP4* (At4g03960, NM_116634.4), *Arabidopsis PFA-DSP5* (At5g16480, NM_121653.4),

Arabidopsis PP2AA3 (At1g13320, NM_101203) and *Arabidopsis TIP41-like* (At3g54000, NM_115260).

Supporting Information

The following supporting information is available.

Figure S1: Purification of PFA-DSP proteins.

Figure S2: *In vitro*, *Arabidopsis* PFA-DSP1 displays robust PP-InsP phosphohydrolase activity against 5-InsP$_7$ and partial phosphohydrolase activity against 4-InsP$_7$ and 6-InsP$_7$, respectively.

Figure S3: In the absence of divalent cations, all InsP$_7$ isomers with the exception of 2-InsP$_7$ become substrates for selected *Arabidopsis* PFA-DSPs *in vitro*.

Figure S4: In the presence of Mg^{2+}, PFA-DSP1 and PFA-DSP3 display robust *in vitro* InsP$_7$ phosphohydrolase activity with high specificity for the 5-β-phosphate.

Figure S5: Under prolonged incubation time, *Arabidopsis* PFA-DSP1 efficiently hydrolyzes 5-InsP$_7$, 4-InsP$_7$ and 6-InsP$_7$ but only displays partial activities against 1-InsP$_7$ and 3-InsP$_7$, and a very weak activity against 2-InsP$_7$.

Figure S6: *Arabidopsis* PFA-DSP1 maintains 5-InsP$_7$ phosphohydrolase activity during prolonged incubation times *in vitro*.

Figure S7: *In vitro*, *Arabidopsis* PFA-DSPs display robust 1/3,5-InsP$_8$ phosphohydrolase activity.

Figure S8: Heterologous expression of *Arabidopsis* PFA-DSPs complements *siw14Δ*-associated defects in InsP$_7$/InsP$_6$ ratios in yeast.

Figure S9: Complementation of *siw14Δ*-associated growth defects depends on catalytic activity.

Figure S10: Single mutant *Arabidopsis pfa-dsp1* loss-of-function lines do not display InsP/PP-InsP defects.

Figure S11: *Arabidopsis* PFA-DSP1, 2 and 4 are strongly induced by P$_i$ deficiency.

Table S1: Oligonucleotide sequences.

Author Contributions

D.L., G.S., and P.G. conceived the study. P.G., D.L., G.S., H.J.J., and R.F.H.G. designed experiments. P.G., R.S., D.L., G.L. D.Q., J.W., M.H., N.J., K.R., J.S., N.F.R., R.F.H.G. performed experiments. P.G. generated yeast mutants and performed all yeast experiments, generated constructs, isolated T-DNA insertion lines, performed HPLC analyses of plants, performed qPCR analyses, performed plant infiltration and TiO_2 pulldowns and analysed most of the experiments. R.S. purified recombinant proteins and carried out and analysed *in vitro* kinase assays. G.L. and D.Q. performed CE-ESI-MS/MS analysis and isomer identification. J.W. and J.S. generated constructs and established the expression and purification of recombinant proteins. N. J., M.H., and K.R. synthesized $InsP_7$ and $InsP_8$ isomers. N.F.R. isolated T-DNA insertion lines, performed HPLC analyses of plants, generated constructs and performed qPCR analyses. R.F.H.G. generated plant samples for CE-ESI-MS analysis and did transcriptome analysis. M.N.T. synthesized ^{13}C-InsP standards. V.G. analysed and quantified HPLC analyses. P.G., G.S., D.L., H.J.J. and D.F. supervised the experimental work. P.G., G.S., R.S., D.L., and R.Y. wrote the manuscript with input from all authors.

Notes

The authors declare no competing financial interest.

Acknowledgments

Funding Sources

&Present address: Department of Biomedicine, University of Basel, 4058 Basel, Switzerland

References

1. Menniti, F. S., Miller, R. N., Putney, J. W., Jr., and Shears, S. B. (1993) Turnover of inositol polyphosphate pyrophosphates in pancreatoma cells, J Biol Chem 268, 3850-3856.
2. Stephens, L., Radenberg, T., Thiel, U., Vogel, G., Khoo, K. H., Dell, A., Jackson, T. R., Hawkins, P. T., and Mayr, G. W. (1993) The detection, purification, structural characterization, and metabolism of diphosphoinositol pentakisphosphate(s) and bisdiphosphoinositol tetrakisphosphate(s), J Biol Chem 268, 4009-4015.
3. Thota, S. G., and Bhandari, R. (2015) The emerging roles of inositol pyrophosphates in eukaryotic cell physiology, J Biosciences 40, 593-605.
4. Shears, S. B. (2018) Intimate connections: Inositol pyrophosphates at the interface of metabolic regulation and cell signaling, Journal of Cellular Physiology 233, 1897-1912.
5. Laha, D., Johnen, P., Azevedo, C., Dynowski, M., Weiss, M., Capolicchio, S., Mao, H., Iven, T., Steenbergen, M., Freyer, M., Gaugler, P., de Campos, M. K., Zheng, N., Feussner, I., Jessen, H. J., Van Wees, S. C., Saiardi, A., and Schaaf, G. (2015) VIH2 Regulates the Synthesis of Inositol Pyrophosphate InsP8 and Jasmonate-Dependent Defenses in Arabidopsis, Plant Cell 27, 1082-1097.
6. Laha, D., Parvin, N., Dynowski, M., Johnen, P., Mao, H., Bitters, S. T., Zheng, N., and Schaaf, G. (2016) Inositol Polyphosphate Binding Specificity of the Jasmonate Receptor Complex, Plant Physiol 171, 2364-2370.
7. Wild, R., Gerasimaite, R., Jung, J. Y., Truffault, V., Pavlovic, I., Schmidt, A., Saiardi, A., Jessen, H. J., Poirier, Y., Hothorn, M., and Mayer, A. (2016) Control of eukaryotic phosphate homeostasis by inositol polyphosphate sensor domains, Science.
8. Couso, I., Evans, B., Li, J., Liu, Y., Ma, F., Diamond, S., Allen, D. K., and Umen, J. G. (2016) Synergism between inositol polyphosphates and TOR kinase signaling in nutrient sensing, growth control and lipid metabolism in Chlamydomonas, Plant Cell.
9. Dong, J., Ma, G., Sui, L., Wei, M., Satheesh, V., Zhang, R., Ge, S., Li, J., Zhang, T. E., Wittwer, C., Jessen, H. J., Zhang, H., An, G. Y., Chao, D. Y., Liu, D., and Lei, M. (2019) Inositol Pyrophosphate InsP8 Acts as an Intracellular Phosphate Signal in Arabidopsis, Mol Plant 12, 1463-1473.
10. Zhu, J., Lau, K., Puschmann, R., Harmel, R. K., Zhang, Y., Pries, V., Gaugler, P., Broger, L., Dutta, A. K., Jessen, H. J., Schaaf, G., Fernie, A. R., Hothorn, L. A., Fiedler, D., and Hothorn, M. (2019) Two bifunctional inositol pyrophosphate kinases/phosphatases control plant phosphate homeostasis, Elife 8.
11. Riemer, E., Qiu, D., Laha, D., Harmel, R. K., Gaugler, P., Gaugler, V., Frei, M., Hajirezaei, M. R., Laha, N. P., Krusenbaum, L., Schneider, R., Saiardi, A., Fiedler, D., Jessen, H. J., Schaaf, G., and Giehl, R. F. H. (2021) ITPK1 is an InsP6/ADP phosphotransferase that controls phosphate signaling in Arabidopsis, Mol Plant.
12. Gulabani, H., Goswami, K., Walia, Y., Roy, A., Noor, J. J., Ingole, K. D., Kasera, M., Laha, D., Giehl, R. F. H., Schaaf, G., and Bhattacharjee, S. (2021) Arabidopsis inositol polyphosphate kinases

IPK1 and ITPK1 modulate crosstalk between SA-dependent immunity and phosphate-starvation responses, Plant Cell Rep.

13. Laha, N. P., Dhir, Y. W., Giehl, R. F. H., Schäfer, E. M., Gaugler, P., Shishavan, Z. H., Gulabani, H., Mao, H., Zheng, N., von Wirén, N., Jessen, H. J., Saiardi, A., Bhattacharjee, S., Laha, D., and Schaaf, G. (2020) ITPK1-Dependent Inositol Polyphosphates Regulate Auxin Responses in Arabidopsis thaliana, bioRxiv.

14. Lin, H., Fridy, P. C., Ribeiro, A. A., Choi, J. H., Barma, D. K., Vogel, G., Falck, J. R., Shears, S. B., York, J. D., and Mayr, G. W. (2009) Structural analysis and detection of biological inositol pyrophosphates reveal that the family of VIP/diphosphoinositol pentakisphosphate kinases are 1/3-kinases, J Biol Chem 284, 1863-1872.

15. Mulugu, S., Bai, W., Fridy, P. C., Bastidas, R. J., Otto, J. C., Dollins, D. E., Haystead, T. A., Ribeiro, A. A., and York, J. D. (2007) A conserved family of enzymes that phosphorylate inositol hexakisphosphate, Science 316, 106-109.

16. Saiardi, A., Erdjument-Bromage, H., Snowman, A. M., Tempst, P., and Snyder, S. H. (1999) Synthesis of diphosphoinositol pentakisphosphate by a newly identified family of higher inositol polyphosphate kinases, Curr Biol 9, 1323-1326.

17. Wang, H., Falck, J. R., Hall, T. M., and Shears, S. B. (2011) Structural basis for an inositol pyrophosphate kinase surmounting phosphate crowding, Nat Chem Biol 8, 111-116.

18. Laha, D., Kamleitner, M., Johnen, P., and Schaaf, G. (2021) Analyses of Inositol Phosphates and Phosphoinositides by Strong Anion Exchange (SAX)-HPLC, Methods Mol Biol 2295, 365-378.

19. Qiu, D. Y., Eisenbeis, V. B., Saiardi, A., and Jessen, H. J. (2021) Absolute Quantitation of Inositol Pyrophosphates by Capillary Electrophoresis Electrospray Ionization Mass Spectrometry, Jove-J Vis Exp.

20. Desai, M., Rangarajan, P., Donahue, J. L., Williams, S. P., Land, E. S., Mandal, M. K., Phillippy, B. Q., Perera, I. Y., Raboy, V., and Gillaspy, G. E. (2014) Two inositol hexakisphosphate kinases drive inositol pyrophosphate synthesis in plants, Plant J 80, 642-653.

21. Flores, S., and Smart, C. C. (2000) Abscisic acid-induced changes in inositol metabolism in Spirodela polyrrhiza, Planta 211, 823-832.

22. Lemtiri-Chlieh, F., MacRobbie, E. A., and Brearley, C. A. (2000) Inositol hexakisphosphate is a physiological signal regulating the K+-inward rectifying conductance in guard cells, Proc Natl Acad Sci U S A 97, 8687-8692.

23. Qiu, D. Y., Wilson, M. S., Eisenbeis, V. B., Harmel, R. K., Riemer, E., Haas, T. M., Wittwer, C., Jork, N., Gu, C. F., Shears, S. B., Schaaf, G., Kammerer, B., Fiedler, D., Saiardi, A., and Jessen, H. J. (2020) Analysis of inositol phosphate metabolism by capillary electrophoresis electrospray ionization mass spectrometry, Nature communications 11.

24. Laha, D., Parvin, N., Hofer, A., Giehl, R. F. H., Fernandez-Rebollo, N., von Wiren, N., Saiardi, A., Jessen, H. J., and Schaaf, G. (2019) Arabidopsis ITPK1 and ITPK2 Have an Evolutionarily Conserved Phytic Acid Kinase Activity, ACS chemical biology 14, 2127-2133.

25. Adepoju, O., Williams, S. P., Craige, B., Cridland, C. A., Sharpe, A. K., Brown, A. M., Land, E., Perera, I. Y., Mena, D., Sobrado, P., and Gillaspy, G. E. (2019) Inositol Trisphosphate Kinase and Diphosphoinositol Pentakisphosphate Kinase Enzymes Constitute the Inositol Pyrophosphate Synthesis Pathway in Plants, bioRxiv.

26. Whitfield, H., White, G., Sprigg, C., Riley, A. M., Potter, B. V. L., Hemmings, A. M., and Brearley, C. A. (2020) An ATP-responsive metabolic cassette comprised of inositol tris/tetrakisphosphate kinase 1 (ITPK1) and inositol pentakisphosphate 2-kinase (IPK1) buffers diphosphophoinositol phosphate levels, Biochemical Journal 477, 2621-2638.

27. Wang, Z. R., Kuo, H. F., and Chiou, T. J. (2021) Intracellular phosphate sensing and regulation of phosphate transport systems in plants, Plant Physiology 187, 2043-2055.

28. Ried, M. K., Wild, R., Zhu, J. S., Pipercevic, J., Sturm, K., Broger, L., Harmel, R. K., Abriata, L. A., Hothorn, L. A., Fiedler, D., Hiller, S., and Hothorn, M. (2021) Inositol pyrophosphates

promote the interaction of SPX domains with the coiled-coil motif of PHR transcription factors to regulate plant phosphate homeostasis, Nature communications 12.

29. Gerasimaite, R., Pavlovic, I., Capolicchio, S., Hofer, A., Schmidt, A., Jessen, H. J., and Mayer, A. (2017) Inositol Pyrophosphate Specificity of the SPX-Dependent Polyphosphate Polymerase VTC, ACS chemical biology 12, 648-653.

30. Zhou, J., Hu, Q., Xiao, X., Yao, D., Ge, S., Ye, J., Li, H., Cai, R., Liu, R., Meng, F., Wang, C., Zhu, J. K., Lei, M., and Xing, W. (2021) Mechanism of phosphate sensing and signaling revealed by rice SPX1-PHR2 complex structure, Nature communications 12, 7040.

31. Rubio, V., Linhares, F., Solano, R., Martin, A. C., Iglesias, J., Leyva, A., and Paz-Ares, J. (2001) A conserved MYB transcription factor involved in phosphate starvation signaling both in vascular plants and in unicellular algae, Gene Dev 15, 2122-2133.

32. Bustos, R., Castrillo, G., Linhares, F., Puga, M. I., Rubio, V., Perez-Perez, J., Solano, R., Leyva, A., and Paz-Ares, J. (2010) A Central Regulatory System Largely Controls Transcriptional Activation and Repression Responses to Phosphate Starvation in Arabidopsis, PLoS genetics 6.

33. Puga, M. I., Mateos, I., Charukesi, R., Wang, Z., Franco-Zorrilla, J. M., de Lorenzo, L., Irigoye, M. L., Masiero, S., Bustos, R., Rodriguez, J., Leyva, A., Rubio, V., Sommer, H., and Paz-Ares, J. (2014) SPX1 is a phosphate-dependent inhibitor of PHOSPHATE STARVATION RESPONSE 1 in Arabidopsis, P Natl Acad Sci USA 111, 14947-14952.

34. Fridy, P. C., Otto, J. C., Dollins, D. E., and York, J. D. (2007) Cloning and characterization of two human VIP1-like inositol hexakisphosphate and diphosphoinositol pentakisphosphate kinases, J Biol Chem 282, 30754-30762.

35. Wang, H., Nair, V. S., Holland, A. A., Capolicchio, S., Jessen, H. J., Johnson, M. K., and Shears, S. B. (2015) Asp1 from Schizosaccharomyces pombe binds a [2Fe-2S](2+) cluster which inhibits inositol pyrophosphate 1-phosphatase activity, Biochemistry 54, 6462-6474.

36. Pascual-Ortiz, M., Saiardi, A., Walla, E., Jakopec, V., Kunzel, N. A., Span, I., Vangala, A., and Fleig, U. (2018) Asp1 Bifunctional Activity Modulates Spindle Function via Controlling Cellular Inositol Pyrophosphate Levels in Schizosaccharomyces pombe, Mol Cell Biol 38.

37. Kilari, R. S., Weaver, J. D., Shears, S. B., and Safrany, S. T. (2013) Understanding inositol pyrophosphate metabolism and function: Kinetic characterization of the DIPPs, Febs Letters 587, 3464-3470.

38. Caffrey, J. J., Hidaka, K., Matsuda, M., Hirata, M., and Shears, S. B. (1999) The human and rat forms of multiple inositol polyphosphate phosphatase: functional homology with a histidine acid phosphatase up-regulated during endochondral ossification, Febs Letters 442, 99-104.

39. Safrany, S. T., Ingram, S. W., Cartwright, J. L., Falck, J. R., McLennan, A. G., Barnes, L. D., and Shears, S. B. (1999) The diadenosine hexaphosphate hydrolases from Schizosaccharomyces pombe and Saccharomyces cerevisiae are homologues of the human diphosphoinositol polyphosphate phosphohydrolase - Overlapping substrate specificities in a MutT-type protein, Journal of Biological Chemistry 274, 21735-21740.

40. Andreeva, N., Ledova, L., Ryazanova, L., Tomashevsky, A., Kulakovskaya, T., and Eldarov, M. (2019) Ppn2 endopolyphosphatase overexpressed in Saccharomyces cerevisiae: Comparison with Ppn1, Ppx1, and Ddp1 polyphosphatases, Biochimie 163, 101-107.

41. Lonetti, A., Szijgyarto, Z., Bosch, D., Loss, O., Azevedo, C., and Saiardi, A. (2011) Identification of an Evolutionarily Conserved Family of Inorganic Polyphosphate Endopolyphosphatases, Journal of Biological Chemistry 286, 31966-31974.

42. Steidle, E. A., Chong, L. S., Wu, M., Crooke, E., Fiedler, D., Resnick, A. C., and Rolfes, R. J. (2016) A Novel Inositol Pyrophosphate Phosphatase in Saccharomyces cerevisiae: Siw14 PROTEIN SELECTIVELY CLEAVES THE beta-PHOSPHATE FROM 5-DIPHOSPHOINOSITOL PENTAKISPHOSPHATE (5PP-IP5), J Biol Chem 291, 6772-6783.

43. Wang, H., Gu, C., Rolfes, R. J., Jessen, H. J., and Shears, S. B. (2018) Structural and biochemical characterization of Siw14: A protein-tyrosine phosphatase fold that metabolizes inositol pyrophosphates, J Biol Chem 293, 6905-6914.

44. Roma-Mateo, C., Sacristan-Reviriego, A., Beresford, N. J., Caparros-Martin, J. A., Culianez-Macia, F. A., Martin, H., Molina, M., Tabernero, L., and Pulido, R. (2011) Phylogenetic and genetic linkage between novel atypical dual-specificity phosphatases from non-metazoan organisms, Molecular Genetics and Genomics 285, 341-354.

45. Roma-Mateo, C., Rios, P., Tabernero, L., Attwood, T. K., and Pulido, R. (2007) A novel phosphatase family, structurally related to dual-specificity phosphatases, that displays unique amino acid sequence and substrate specificity, Journal of Molecular Biology 374, 899-909.

46. Aceti, D. J., Bitto, E., Yakunin, A. F., Proudfoot, M., Bingman, C. A., Frederick, R. O., Sreenath, H. K., Vojtik, F. C., Wrobel, R. L., Fox, B. G., Markley, J. L., and Phillips, G. N. (2008) Structural and functional characterization of a novel phosphatase from the Arabidopsis thaliana gene locus At1g05000, Proteins-Structure Function and Bioinformatics 73, 241-253.

47. Irvine, R. F., and Schell, M. J. (2001) Back in the water: the return of the inositol phosphates, Nat Rev Mol Cell Biol 2, 327-338.

48. Blüher, D., Laha, D., Thieme, S., Hofer, A., Eschen-Lippold, L., Masch, A., Balcke, G., Pavlovic, I., Nagel, O., Schonsky, A., Hinkelmann, R., Wörner, J., Parvin, N., Greiner, R., Weber, S., Tissier, A., Schutkowski, M., Lee, J., Jessen, H., Schaaf, G., and Bonas, U. (2017) A 1-phytase type III effector interferes with plant hormone signaling, Nature communications 8, 2159.

49. Arcaro, A., and Wymann, M. P. (1993) Wortmannin is a potent phosphatidylinositol 3-kinase inhibitor: the role of phosphatidylinositol 3,4,5-trisphosphate in neutrophil responses, Biochem J 296 (Pt 2), 297-301.

50. Saiardi, A., Resnick, A. C., Snowman, A. M., Wendland, B., and Snyder, S. H. (2005) Inositol pyrophosphates regulate cell death and telomere length through phosphoinositide 3-kinase-related protein kinases, Proc Natl Acad Sci U S A 102, 1911-1914.

51. Estevez, F., Pulford, D., Stark, M. J., Carter, A. N., and Downes, C. P. (1994) Inositol trisphosphate metabolism in Saccharomyces cerevisiae: identification, purification and properties of inositol 1,4,5-trisphosphate 6-kinase, Biochemical Journal 302, 709-716.

52. Kuo, H. F., Hsu, Y. Y., Lin, W. C., Chen, K. Y., Munnik, T., Brearley, C. A., and Chiou, T. J. (2018) Arabidopsis inositol phosphate kinases IPK1 and ITPK1 constitute a metabolic pathway in maintaining phosphate homeostasis, Plant J.

53. Stevenson-Paulik, J., Bastidas, R. J., Chiou, S. T., Frye, R. A., and York, J. D. (2005) Generation of phytate-free seeds in Arabidopsis through disruption of inositol polyphosphate kinases, Proc Natl Acad Sci U S A 102, 12612-12617.

54. Safrany, S. T., Caffrey, J. J., Yang, X., Bembenek, M. E., Moyer, M. B., Burkhart, W. A., and Shears, S. B. (1998) A novel context for the 'MutT' module, a guardian of cell integrity, in a diphosphoinositol polyphosphate phosphohydrolase, EMBO J 17, 6599-6607.

55. Gruber, B. D., Giehl, R. F., Friedel, S., and von Wiren, N. (2013) Plasticity of the Arabidopsis root system under nutrient deficiencies, Plant Physiol.

56. Loque, D., Lalonde, S., Looger, L. L., von Wiren, N., and Frommer, W. B. (2007) A cytosolic trans-activation domain essential for ammonium uptake, Nature 446, 195-198.

57. Nakamura, S., Mano, S., Tanaka, Y., Ohnishi, M., Nakamori, C., Araki, M., Niwa, T., Nishimura, M., Kaminaka, H., Nakagawa, T., Sato, Y., and Ishiguro, S. (2010) Gateway Binary Vectors with the Bialaphos Resistance Gene, <I>bar</I>, as a Selection Marker for Plant Transformation, Bioscience, Biotechnology, and Biochemistry 74, 1315-1319.

58. Gueldener, U., Heinisch, J., Koehler, G. J., Voss, D., and Hegemann, J. H. (2002) A second set of loxP marker cassettes for Cre-mediated multiple gene knockouts in budding yeast, Nucleic Acids Res 30, e23.

59. Onnebo, S. M., and Saiardi, A. (2009) Inositol pyrophosphates modulate hydrogen peroxide signalling, Biochem J 423, 109-118.

60. Gietz, R. D., Schiestl, R. H., Willems, A. R., and Woods, R. A. (1995) Studies on the transformation of intact yeast cells by the LiAc/SS-DNA/PEG procedure, Yeast 11, 355-360.

61. Zonneveld, B. J. M. (1986) B.J.M. Zonneveld. 1986. Cheap and simple yeast media. J. Microb. Meth. 4: 287-91, Journal of Microbiological Methods - J MICROBIOL METH 4.

62. Schaaf, G., Betts, L., Garrett, T. A., Raetz, C. R., and Bankaitis, V. A. (2006) Crystallization and preliminary X-ray diffraction analysis of phospholipid-bound Sfh1p, a member of the *Saccharomyces cerevisiae* Sec14p-like phosphatidylinositol transfer protein family, Acta Crystallogr Sect F Struct Biol Cryst Commun 62, 1156-1160.

63. Capolicchio, S., Thakor, D. T., Linden, A., and Jessen, H. J. (2013) Synthesis of unsymmetric diphospho-inositol polyphosphates, Angewandte Chemie 52, 6912-6916.

64. Capolicchio, S., Wang, H., Thakor, D. T., Shears, S. B., and Jessen, H. J. (2014) Synthesis of Densely Phosphorylated Bis-1,5-Diphospho-myo-Inositol Tetrakisphosphate and its Enantiomer by Bidirectional P-Anhydride Formation, Angewandte Chemie.

65. Azevedo, C., and Saiardi, A. (2006) Extraction and analysis of soluble inositol polyphosphates from yeast, Nat Protoc 1, 2416-2422.

66. Gaugler, P., Gaugler, V., Kamleitner, M., and Schaaf, G. (2020) Extraction and Quantification of Soluble, Radiolabeled Inositol Polyphosphates from Different Plant Species using SAX-HPLC, J Vis Exp.